pubs.acs.org/acschemicalbiology

Articles

Global Protease Activity Profiling Identifies HER2-Driven Proteolysis in Breast Cancer

Eugenia C. Salcedo, Michael B. Winter, Natalia Khuri, Giselle M. Knudsen, Andrej Sali, and Charles S. Craik*

Cite This: *ACS Chem. Biol.* 2021, 16, 712–723

Read Online

ABSTRACT: Differential expression of extracellular proteases and endogenous protease inhibitors has been associated with distinct molecular subtypes of breast cancer. However, due to the tight post-translational regulation of protease activity, protease expression-level data alone are not sufficient to understand the role of proteases in malignant transformation. Therefore, we hypothesized that global profiles of extracellular protease activity could more completely reflect differences observed at the transcriptional level in breast cancer and that subtype-associated protease activity may be leveraged to identify specific proteases that play a functional role in cancer signaling. Here, we used a global peptide library-based approach to profile the activities of proteases within distinct breast cancer subtypes. Analysis of 3651 total peptide cleavages from a panel of well-characterized breast cancer cell lines demonstrated differences in proteolytic signatures between cell lines. Cell line clustering based on protease cleavages within the peptide library expanded upon the expected classification derived from transcriptional profiling. An isogenic cell line model developed to further interrogate proteolysis in the HER2 subtype revealed a proteolytic signature consistent with activation of TGF-β signaling. Specifically, we determined that a metalloprotease involved in TGF-β signaling, BMP1, was upregulated at both the protein (2-fold, $P = 0.001$) and activity ($P = 0.0599$) levels. Inhibition of BMP1 and HER2 suppressed invasion of HER2-expressing cells by 35% ($P < 0.0001$), compared to 15% ($P = 0.0086$) observed in cells where only HER2 was inhibited. In summary, through global identification of extracellular proteolysis in breast cancer cell lines, we demonstrate subtype-specific differences in protease activity and elucidate proteolysis associated with HER2-mediated signaling.

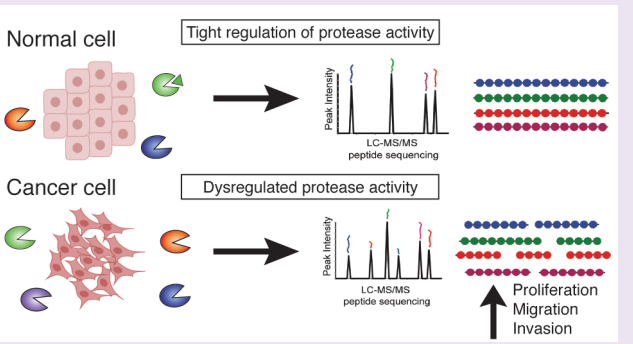

Breast cancer is a highly complex disease composed of multiple molecular subtypes that display unique clinical outcomes and response to treatment.[1,2] Traditional classification of breast cancer by immunohistochemistry (IHC) has been based on estrogen receptor (ER), progesterone receptor (PR), and HER2 (*ERBB2*) receptor expression.[3,4] Absence of these markers is known as triple negative breast cancer (TNBC).[3,4] TNBC is associated with a more aggressive phenotype and has a worse prognosis than receptor-positive subtypes.[5] IHC markers are routinely used in the clinic for diagnosis and as predictors of therapeutic response;[6] however, given the complexity of the disease, individual markers sometimes provide limited information about the underlying mechanisms and appropriate targeted therapy.

Genome-wide transcriptional analysis of breast tumors and cancer cell lines has allowed for a better understanding of the molecular mechanisms dysregulated in the disease.[7−9] Differential expression of previously known and novel genes has resulted in further refinement of breast cancer groups with most studies classifying breast cancer into three major molecular subtypes: luminal (positive for ER, PR, and/or HER2-positive); HER2-positive, in which the receptor is overexpressed or amplified; and basal-like, which is usually triple negative for the receptors.[7−9] In addition to genes involved in cell cycle regulation and differentiation such as *TP53* and *GATA3*, proteases and protease inhibitors have been found to be differentially expressed in breast cancer subtypes. For example, expression of the serine proteases *KLK5*, *KLK6*, and *KLK8* were found to be associated with a subgroup of basal-like cell lines termed basal A.[9] Further studies have identified elevated levels of the serine protease urokinase plasminogen activator or uPA (*PLAU*) and its receptor uPAR (*PLAUR*) in basal-like cell lines.[9,10] In addition, high levels of uPA and its cognate inhibitor PAI-1 have been clinically validated as prognostic biomarkers for lymph-node negative breast cancer and correlate with poor disease-free survival.[11]

Received: December 30, 2020
Accepted: March 16, 2021
Published: March 25, 2021

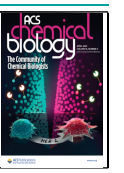

https://doi.org/10.1021/acschembio.0c01000
ACS Chem. Biol. 2021, 16, 712–723

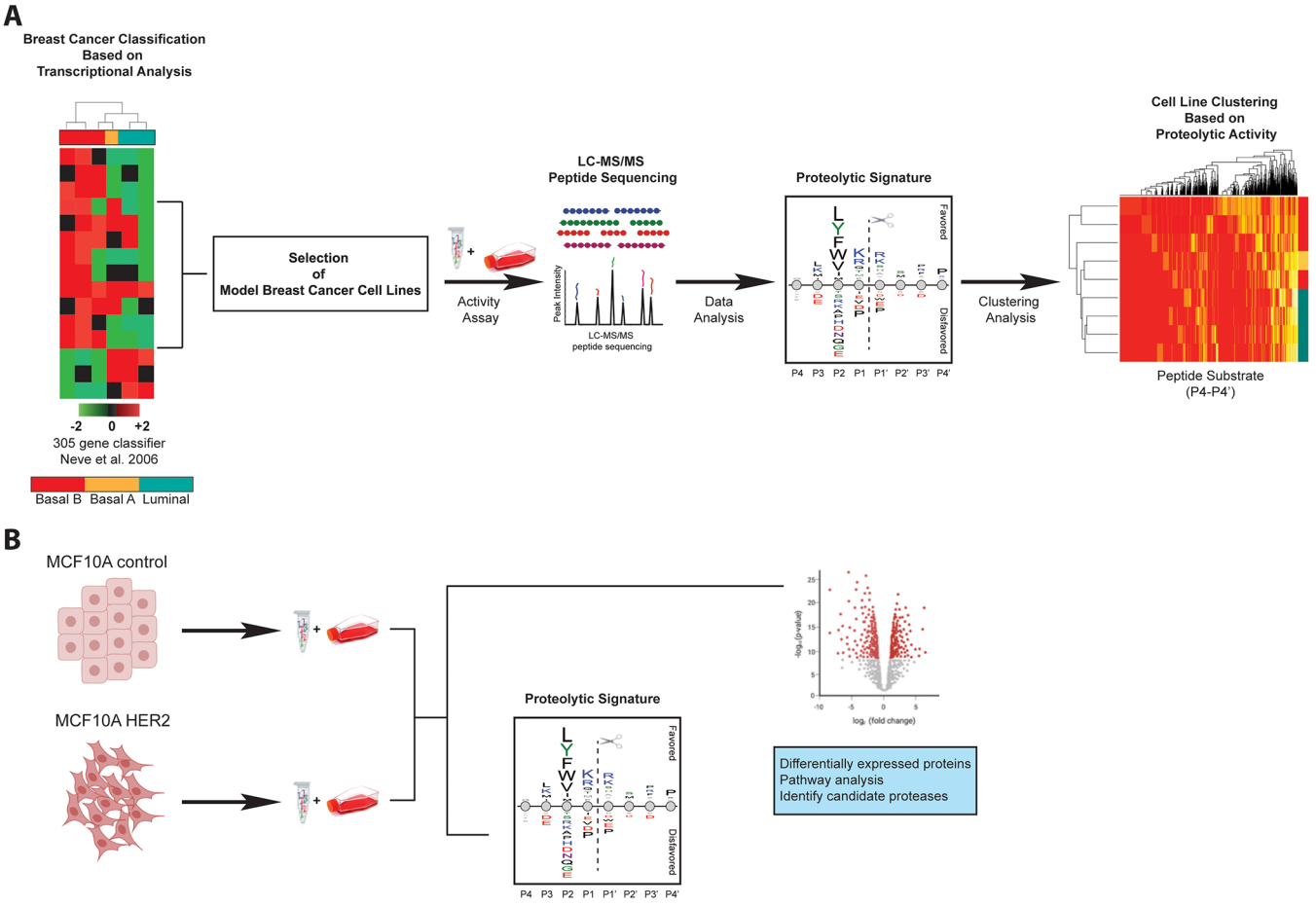

Figure 1. Evaluating the role of extracellular proteolysis in breast cancer subtypes. (A) Analysis of protease activity in model breast cancer cell lines of distinct molecular subgroups. (B) Analysis of HER2-associated proteolysis in breast cancer using an isogenic cell line model. Created with BioRender.

However, the impact of such changes in gene or protein expression on global protease activity within breast cancer remains poorly explored.

In normal tissues, proteolysis is tightly regulated at the post-translational level with most proteases synthesized as inactive zymogens requiring the removal of a propeptide for enzymatic activity.[12] In addition, proteolytic activity is regulated by the presence of endogenous protease inhibitors and changes in subcellular localization.[12] In contrast to normal tissues, dysregulation of proteolysis has been linked to the initiation and progression of cancer.[13−15] For example, increased activity of the transmembrane serine protease, matriptase, due to reduced relative levels of its cognate inhibitor, HAI-1, has been associated with malignant progression in colon cancer.[16] In addition, lysosomal cysteine proteases, such as cathepsin B in breast cancer, have been found to be mislocalized to the extracellular space where they trigger invasion and metastasis.[17] An increasing body of evidence demonstrates that proteases play a highly complex role in cancer progression not only through degradation of extracellular matrix proteins but also participation in numerous proteolytic signaling pathways.[17]

Given the high degree of post-translational regulation of proteases, we hypothesized that protease activity could more completely reflect changes in the functional proteome than protease and/or inhibitor expression levels alone. Here, we used a mass-spectrometry-based approach to identify extracellular protease activity in a global and unbiased manner. To this end, a physiochemically diverse library of 228 synthetic peptide substrates[18,19] was exposed to the secretome of a panel of well-characterized breast cancer cell lines from distinct molecular subtypes (Figure 1A, Table 1). Analysis of 3651 total cleavages from all cell lines revealed differences in global proteolytic signatures. Cell line clustering based on peptide cleavages both supported and expanded upon the expected classification derived from transcriptional analysis. Next, we focused our efforts within the HER2 subtype to identify signaling pathways driving protease activity in HER2-positive breast cancer using an isogenic cell line model (Figure 1B).

Table 1. Selection of Cell Lines to Study Extracellular Proteolysis in Breast Cancer

cell line	gene cluster	intrinsic subtype	ER	PR	HER2
BT-549	basal B	basal	−	−	−
MDA-MB-436	basal B	basal	−	−	−
MDA-MB-231	basal B	basal	−	−	−
MDA-MB-435	basal B	HER2	−	−	+
MDA-MB-468	basal A	basal	−	−	−
SK-BR-3	luminal	HER2	−	−	+
MCF7	luminal	luminal A	+	+	−
BT-474	luminal	luminal B	+	+	+
MDA-MB-453	luminal	HER2	−	−	+

https://doi.org/10.1021/acschembio.0c01000
ACS Chem. Biol. 2021, 16, 712−723

HER2 expression revealed changes consistent with activation of transforming growth factor beta (TGF-β) signaling. We determined that the activity of the metalloprotease BMP1, which is involved in TGF-β signaling was increased in MCF10A HER2-overexpressing cells, and BMP1 inhibition resulted in decreased cellular invasion. Here, we present an approach in which functional subtypes of breast cancer can be identified based on differences in protease activity. We take advantage of these differences to further elucidate a specific protease program associated with HER2-mediated oncogenesis in breast cancer.

RESULTS

Protein Distribution of Extracellular Protease and Inhibitors in Breast Cancer Subtypes. To determine whether gene expression levels for extracellular proteases and inhibitors found to be associated with specific subtypes (Figure S1A) were observed at the protein level as well, we performed proteomic analysis on conditioned media from a panel of nine breast cancer cell lines corresponding to distinct molecular subtypes defined by transcriptional profiling (luminal, basal A, and basal B), including the melanoma cell line MDA-MB-435, previously misidentified as a breast cancer cell line[9,20] (Table 1). Of note, aminopeptidase N (*ANPEP*), a single-pass type II transmembrane protein, previously found to be associated with the basal B subtype by transcriptional profiling,[9] was uniquely detected by proteomics in conditioned media from the basal B cell line BT-549. In addition, uPA (*PLAU*), a secreted serine protease also associated with the basal B subtype, was uniquely detected by proteomics in conditioned media from the basal B cell lines MDA-MB-436 and MDA-MB-231. Further, members of the serine protease kallikrein family, kallikrein-5 and kallikrein-6 (*KLK5*, *KLK6*), previously associated with the basal A subtype at the transcriptional level,[9] were detected by proteomics in conditioned media from the basal A cell line, MDA-MB-468 (Figure S1B, Table S1). Similarly, protease inhibitors differentially expressed at the transcriptional level in breast cancer subgroups were also found to be differentially expressed at the protein level by proteomics. For example, transcriptional upregulation of antileukoproteinase (*SLPI*) and downregulation of cystatin C (*CST3*) in the basal A subtype were observed at the protein level as well (Figure S1, Table S1). Importantly, we also identified aberrant secretion of cathepsin lysosomal cysteine proteases, which could not be predicted from gene expression analysis alone.[9] For example, gene expression levels of cathepsin B show that it is widely expressed in all cell lines, yet secretion of cathepsin B is mostly observed in basal B cell lines (Figure S2, Table S1). Our proteomic analysis of cell line secretomes demonstrated that in many instances proteases and protease inhibitors found to have differential expression at the transcriptional level in specific breast cancer subtypes had differential abundance at the protein level as well, while also highlighting changes in protease protein levels and/or localization not evident by transcriptional analysis alone.

Global Protease Profiling of Breast Cancer Subtypes. Next, we analyzed global changes in extracellular protease activity in the panel of breast cancer cell lines to assess correlation with previously defined genetic subtypes. To identify global profiles of extracellular proteolysis, conditioned media were assayed using a substrate profiling approach termed Multiplex Substrate Profiling by Mass Spectrometry (MSP-MS).[18,19] Matched conditioned media samples were incubated with the MSP-MS library, and time-dependent peptide cleavage products were identified by liquid chromatography tandem mass spectrometry (LC-MS/MS). Analysis of the peptide cleavage products revealed that basal-like cell lines (BT-549, MDA-MB-231, MDA-MB-436, and MDA-MB-468) displayed an overall higher proteolytic activity against the peptide library compared to luminal cell lines (BT-474, SK-BR-3, MCF7, and MDA-MB-453), based on the total number of peptide cleavages observed throughout the assay time course (n = 2053 for basal-like and n = 1254 for luminal at 240 min; Table S2).

To determine whether cell lines associated based on total cleavage events observed against the peptide library, two-way clustering analysis was performed.[21] Clustering results revealed at least three major groups, correlating with previously defined genetic subtypes, while also uncovering potential unique groups based on differences in global protease activity (Figure 2). Luminal cell lines, BT-474, SK-BR-3, MCF7, and MDA-MB-453, grouped together in one cluster (cluster 4) while basal-like cell lines demonstrated more heterogeneous clustering. Basal B cell lines, BT-549 and MDA-MB-436, grouped together in a second cluster (cluster 1), while basal A and basal B cell lines, MDA-MB-468 and MDA-MB-231, grouped together in a third cluster (cluster 3). Interestingly, the melanoma cell line, MDA-MB-435, did not cluster with the others (cluster 2; Figure 2).

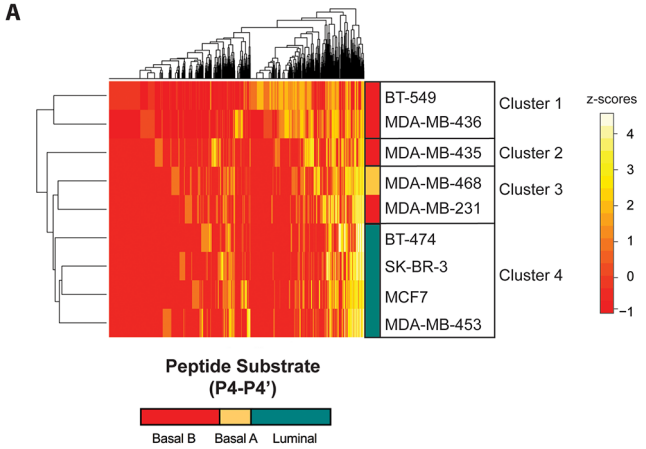

Figure 2. Global analysis of extracellular protease activity in breast cancer subtypes. Conditioned media from breast cancer cell lines of distinct molecular subtypes (luminal, basal A, and basal B) were analyzed for changes in protease activity using the MSP-MS peptide library. (A) Two-way clustering analysis was performed on 3651 total cleavages for all cell lines at 240 min. Clustering results revealed at least three major functional groups based on differences in peptide cleavage within the basal B subtype. Each amino acid of a peptide was encoded using three Hellberg z scores where a positive value indicates cleavage along the peptide. Heatmap rows represent each peptide, and columns represent 24 z scores or descriptors. The color scheme denotes previously defined molecular subtypes: basal B, red; basal A, yellow; and luminal, turquoise. Breast cancer cell lines used and their intrinsic subtype classification are provided (Table 1).

To visualize differences in the substrate specificity profiles of the major four clusters, we generated an iceLogo frequency plot,[22] which considers both cleaved and uncleaved positions in the peptide library, with cleavage occurring between P1 and P1′. Among the shared specificity features identified in the complex conditioned media profiles, all clusters displayed an

https://doi.org/10.1021/acschembio.0c01000
ACS Chem. Biol. 2021, 16, 712−723

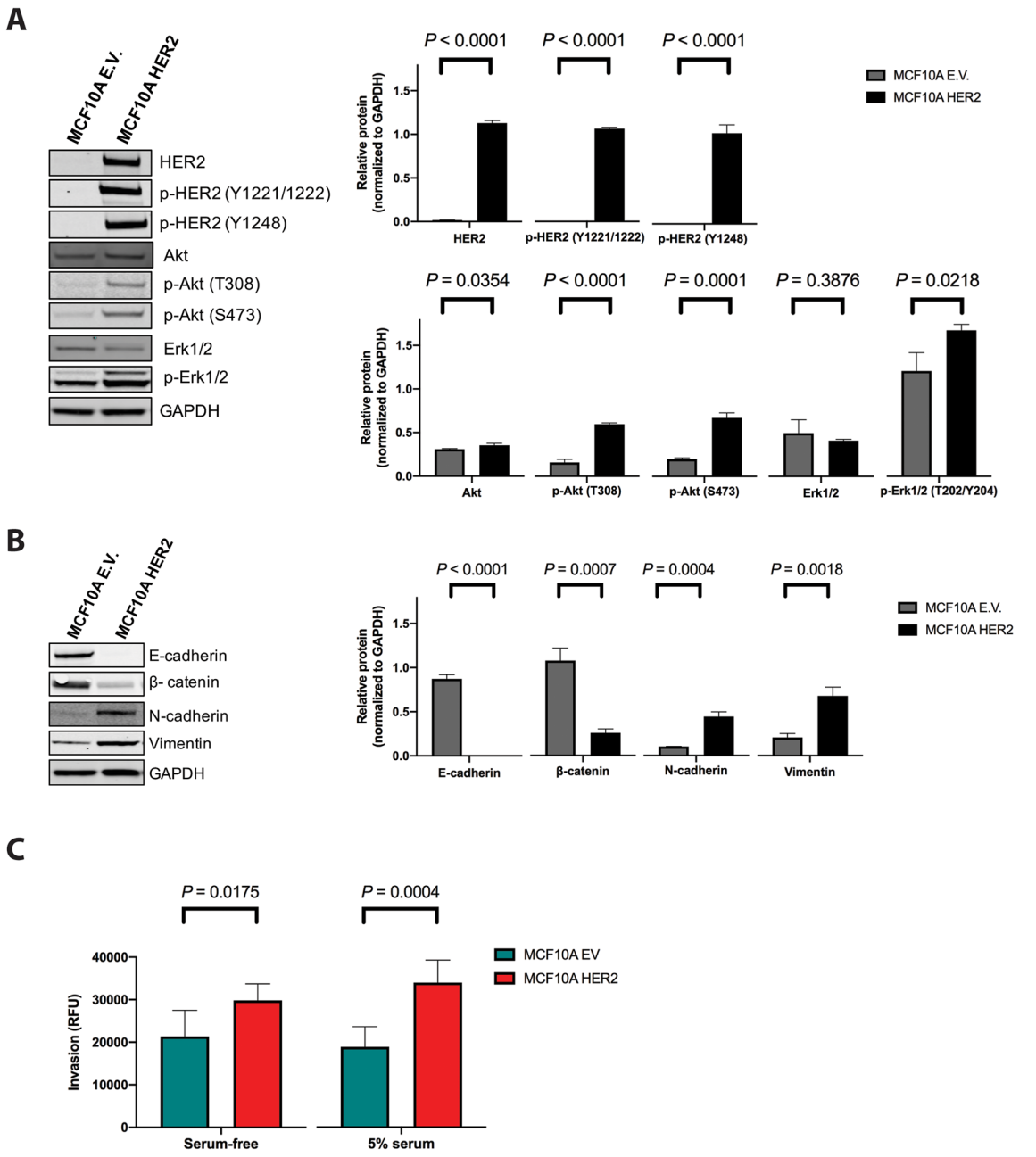

Figure 3. Characterization of an isogenic cell line model of the HER2 subtype. Expression of constitutively active $HER2^{V659E}$ results in activation of downstream signaling pathways and changes consistent with epithelial-to-mesenchymal (EMT) transition. (A) HER2 expression in MCF10A cells leads to activation of PI3K-AKT signaling determined by phosphorylation of AKT at T308 ($P < 0.0001$) and S473 ($P = 0.0001$) and activation of MAPK signaling indicated by phosphorylation of ERK1/2 at T202/Y204 ($P = 0.0218$). (B) HER2 activation resulted in changes consistent with malignant transformation such as downregulation of E-cadherin ($P < 0.0001$) and β-catenin ($P = 0.0007$), as well as upregulation of N-cadherin ($P = 0.0004$) and vimentin ($P = 0.0018$). Signal intensities were normalized to GAPDH protein levels and are reported as mean intensity ± SD. Results are an average of three independent experiments ± SD. (C) HER2 expression resulted in increased invasion *in vitro* across a basement membrane extract with the biggest difference observed using 5% serum as a chemoattractant ($P = 0.0004$). Results for cell invasion are reported as mean RFU ± SD of six wells.

enrichment for bulky hydrophobic or aromatic amino acids at the P1 position (including leucine, norleucine, phenylalanine, tryptophan, or tyrosine). Clusters 3 and 4 demonstrated an enrichment of arginine at the P1 position and several prime-side positions (P1′−P3′). Cluster 4, composed of luminal cell lines, displayed non-prime side specificity not observed in the other clusters with a moderate preference for hydrophobic amino acids, leucine and phenylalanine (P4−P2; Figure S3). Together, our substrate profiling and clustering analysis demonstrate that breast cancer cell lines display distinct protease activity profiles. Future work expanding our analysis to incorporate patient samples can be used to determine whether differences in protease activities may enable activity-based stratification in a more clinically relevant context.

Characterization of an Isogenic Cell Line Model to Study Extracellular Proteolysis in Breast Cancer. Given

https://doi.org/10.1021/acschembio.0c01000
ACS Chem. Biol. 2021, 16, 712−723

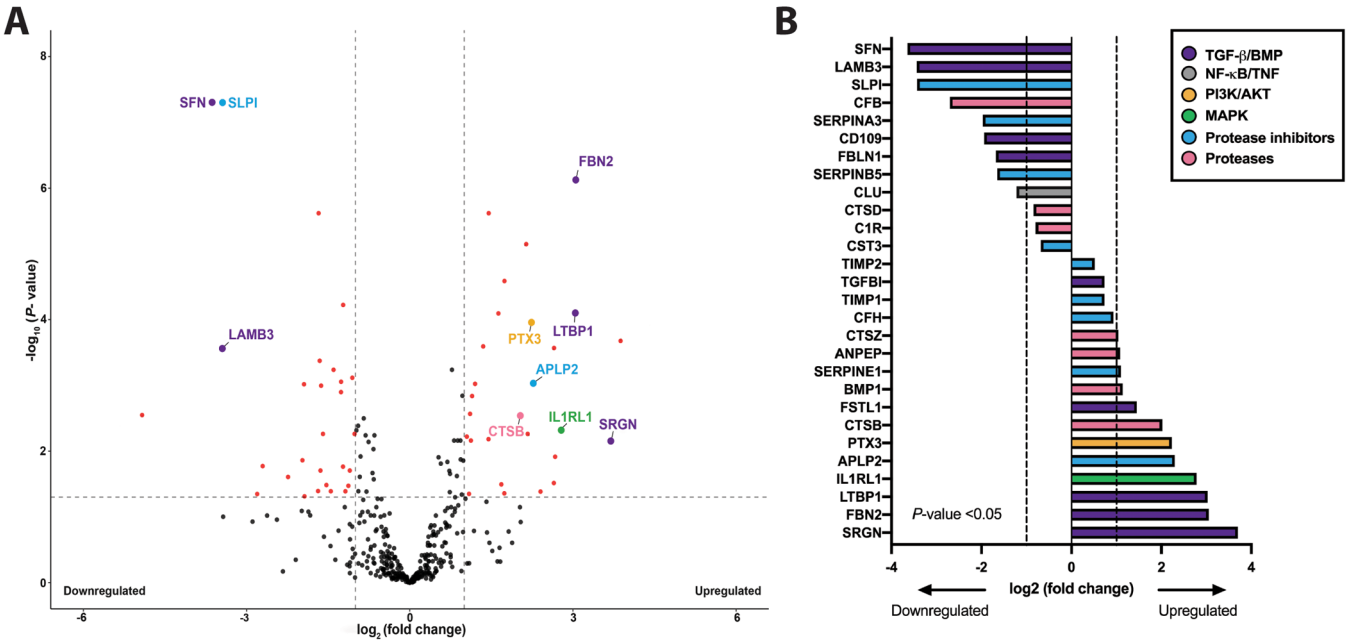

Figure 4. Proteomic analysis of differentially regulated proteins upon HER2 activation. (A) Volcano plot of proteins differentially expressed in MCF10A HER2-expressing cells that were identified by shotgun proteomic analysis of conditioned media. Selected proteases and proteins involved in downstream signaling pathways are highlighted. Trypsin-derived peptides were sequenced by LC-MS/MS and analyzed using MaxQuant. (B) HER2 expression results in differential regulation of proteases, protease inhibitors, and proteins involved in downstream signaling pathways. Downregulation of negative regulators and upregulation of activators involved in TGF-β signaling were identified, suggesting activation of TGF-β signaling in MCF10A HER2 cells. The color scheme on the right denotes proteases, protease inhibitors, and proteins involved in downstream signaling pathways in panels A and B. Differential expression ($\log_2$ fold change, FC) and statistical analysis ($-\log_{10} P$ value) were conducted using MaxQuant protein files in the Bioconductor R package, Proteus. Differential expression was based on analysis of three biological samples and three technical replicates. The significance cutoff was set at $\log_2$ FC $\pm$ 1, $-\log_{10}(P$ value) of 1.3.

the higher degree of heterogeneity observed in basal-like breast tumors compared to luminal subtypes, we chose to further elucidate the regulation of protease activity within HER2-positive breast cancer. To this end, we selected the non-tumorigenic epithelial cell line MCF10A, which has been previously used to study HER2-associated signaling in breast cancer, as an isogenic model for the HER2 subtype.[23] To asses activation of downstream signaling pathways regulated by HER2, MCF10A cells expressing constitutively active HER2 (MCF10A HER2), and MCF10A expressing an empty vector (MCF10A EV) were analyzed by Western blot (Figure 3A). In addition to autophosphorylation, HER2 activation can lead to activation of both the mitogen-activated protein kinase (MAPK) and phosphatidylinositol 3-kinase (PI3K)-AKT pathway.[24] MCF10A HER2 cells showed strong phosphorylation of HER2 Y1221/1222 and Y1248 ($P < 0.0001$). This was accompanied by activation of AKT signaling, notable by phosphorylation of AKT at T308 and S473 ($P < 0.0001$ and $P = 0.0001$, respectively). Activation of MAPK signaling was also observed by increased phosphorylation of ERK1/2 at T202/T204 ($P = 0.0218$; Figure 3A). Taken together, these results confirm that expression of constitutively active HER2 in MCF10A cells results in the expected activation of downstream signaling pathways.

HER2-mediated Oncogenic Transformation Activates Epithelial-to-Mesenchymal Transition (EMT) Programming. Previous studies have demonstrated that constitutive activation of HER2 signaling in MCF10A cells results in oncogenic transformation and activation of the epithelial-to-mesenchymal transition programming (EMT).[23] To this end, we performed Western blot analysis to assess changes in proteins associated with EMT signaling (Figure 3B). HER2 expression in MCF10A cells resulted in downregulation of the epithelial markers E-cadherin ($P < 0.0001$) and β-catenin ($P = 0.0007$), as well as upregulation of mesenchymal markers N-cadherin ($P = 0.0004$) and vimentin ($P = 0.0018$; Figure 3B). EMT is a key event in cancer characterized by a loss of cell-to-cell adhesion and increased invasion,[25,26] and activation of HER2 signaling has been shown to result in increased invasiveness *in vitro*.[27] While HER2 expression did not significantly affect cell proliferation ($P = 0.7723$; Figure S4), it resulted in a significant increase in invasion ($P = 0.0004$; Figure 3C). Taken together, our data show that expression of HER2 in MCF10A cells results in activation of downstream signaling pathways and is consistent with malignant transformation as observed by activation of EMT programming and increased invasion *in vitro*.

Identification of Proteins Differentially Expressed upon HER2-mediated Transformation. To identify proteins differentially regulated in HER2 cells, we performed proteomic analysis on conditioned media from the MCF10A HER2 overexpressing and MCF10A E.V. (control) cells. HER2 expression resulted in differential levels of 55 proteins which included proteases, protease inhibitors, and other proteins involved in regulation of intracellular signaling pathways (Table S3). Three of the top proteins upregulated in MCF10A HER2 cells, serglycin (*SRGN*; 13-fold, $P = 0.007$), fibrillin-2 (*FBN2*; 8-fold, $P = 7.41 \times 10^{-07}$), and latent-transforming growth factor beta-binding protein 1 (*LTBP1*; 8-fold, $P = 8.05 \times 10^{-05}$) are involved in TNF-α and TGF-β pathway activation.[28−30] Interestingly, proteins downregulated by HER2 expression such as 14−3−3 protein sigma (*SFN*;

https://doi.org/10.1021/acschembio.0c01000
ACS Chem. Biol. 2021, 16, 712−723

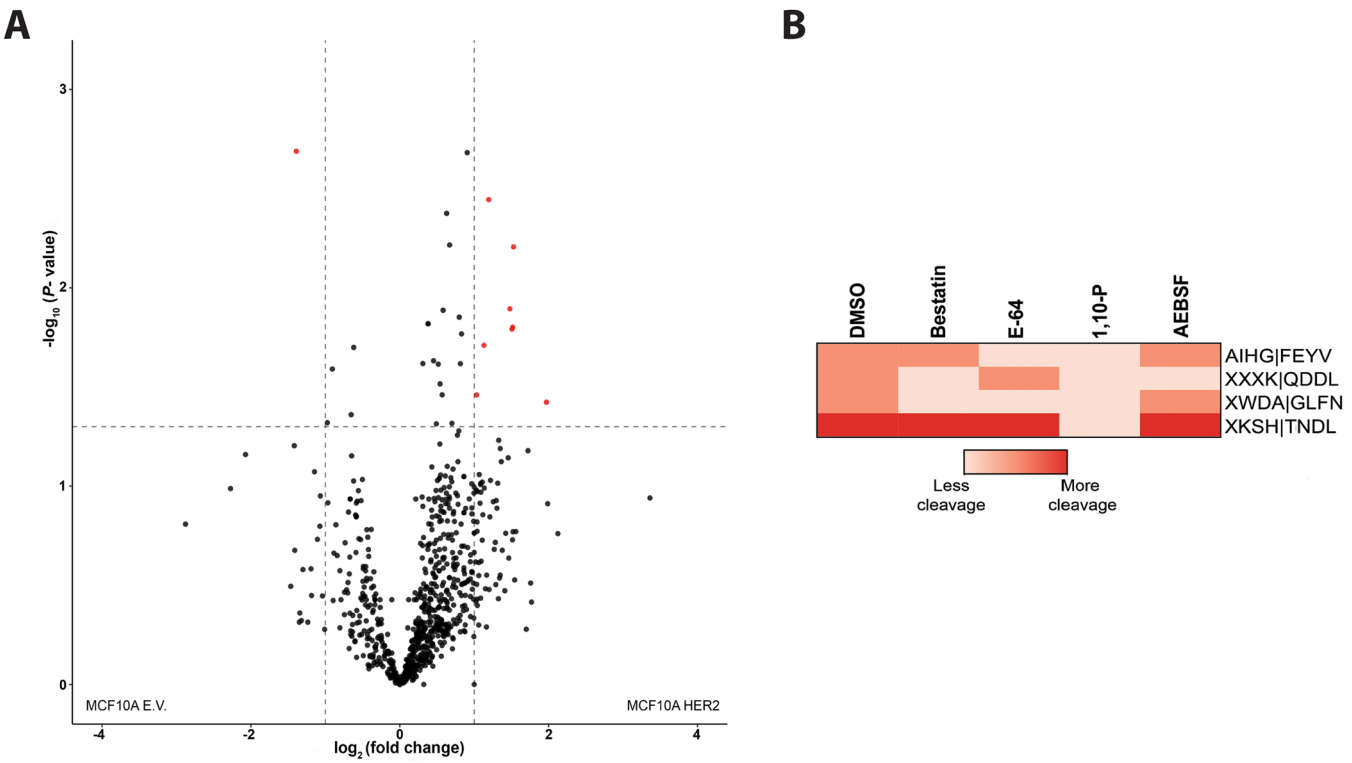

Figure 5. Global analysis of extracellular proteolysis in an isogenic HER2 cell line model. Global analysis of protease activity was performed in conditioned media from MCF10A E.V. (control) and MCF10A HER2 cells using the MSP-MS peptide library. (A) HER2 expression in MCF10A cells resulted in higher proteolytic activity against the peptide library (n = 389 for control and n = 475 for HER2 at 240 min). (B) Pretreatment of conditioned media with protease inhibitors Bestatin, E-64, 1,10-P, and AEBSF revealed predominant metalloprotease activity in both cell lines. Cleavages significantly enriched 2-fold or more in MCF10A HER2 (n = 4, $P < 0.05$) and found in the MSP-MS assay incorporating inhibitors were completely inhibited by 1,10-P. Differentially cleaved peptides ($\log_2$ FC) and statistical analysis ($-\log_{10}$ P value) were conducted using Bioconductor R package limma. For this analysis, peptide cleavages of three independent experiments were used. The significance cutoff was set at $\log_2$ FC ± 1, $-\log_{10}$ (P value) = 1.3.

12.1-fold, $P = 4.99 \times 10^{-08}$), laminin subunit beta-3 (*LAMB3*; 10.6-fold, $P = 0.0003$), CD109 antigen (*CD109*; 3.7-fold, $P = 0.001$), and fibulin-1 (*FBLN1*; 3.2-fold, $P = 2.41 \times 10^{-06}$; Figure 4), mediate the switch of TGF-β from tumor suppressor to tumor promoter, demonstrate involvement in extracellular matrix regulation, and negatively regulate TGF-β pathway activation.[31−33] TGF-β has been previously shown to synergize with oncogenic pathways, and in HER2-overexpressing cells, HER2-TGF-β crosstalk results in increased cell proliferation, cell growth, and invasion.[34] In addition, TGF-β amplifies HER2 signaling by inducing proteolytic cleavage of ErbB ligands into the tumor microenvironment.[35] In turn, HER2 signaling induces the expression and secretion of TGF-β cytokines, creating a positive feedback loop allowing for uncontrolled growth and proliferation.[35,36]

In addition to differential regulation of proteins involved in TGF-β signaling, among the 55 proteins differentially regulated, 12 were found to be proteases or protease inhibitors. Lysosomal cysteine proteases cathepsin B (*CSTB*; 4-fold, $P = 0.003$) and cathepsin Z (*CSTZ*; 2-fold, $P = 0.006$) were found to be significantly upregulated. Downregulation of the serine protease complement factor B (*CFB*; 6.5-fold, $P = 0.002$) and serine protease inhibitors antileukoproteinase (*SLPI*; 10.6-fold, $P = 4.99 \times 10^{-08}$), alpha-1-antichymotrypsin (*SERPINA3*; 3.9-fold, $P = 0.01$), and serpin B5 (*SERPINB5*; 3.2-fold, $P = 0.0004$), a non-inhibitory member of the serine protease inhibitors (SERPINs) family was also observed (Figure 4). Further, consistent with previous studies, the serine protease inhibitor, plasminogen activator inhibitor 1 (*SERPINE1*), a marker of EMT,[37] was upregulated in MCF10A HER2 cells (2.1-fold, $P = 0.003$). Last, the metalloproteases bone morphogenic protein 1 (*BMP1*; 2-fold, $P = 0.001$) and aminopeptidase N (*ANPEP*; 2-fold, $P = 0.009$) were found to be significantly upregulated in MCF10A HER2 cells (Figure 4). Together, our results support the hypothesis that HER2 amplification and/or overexpression activates signaling pathways that may lead to altered proteolysis in HER2-positive breast cancers with higher metastatic potential.[38,39]

Global Analysis of Extracellular Proteolysis Associated with HER2-mediated Transformation. To identify global changes in extracellular proteolysis associated with HER2 expression, conditioned media from MCF10A HER2 overexpression and MCF10A control cell lines were assayed using the MSP-MS peptide library. Comparison of the cleavage profiles revealed that the secretome of MCF10A HER2 cells displayed differential activity against the peptide library (Figures 5A, S5). To identify the protease classes responsible for the major activity observed in both cell lines, broad-spectrum protease inhibitors were incorporated into the MSP-MS assay. Pretreatment of conditioned media with the metalloprotease inhibitor, 1,10-phenanthroline (1,10-P), reduced the total number of cleavages observed by 87% from the MCF10A control cells and 88% from MCF10A HER2 overexpression cells, indicating that metalloproteases were the most active in both cell lines (Table S4). Cleavages significantly enriched 2-fold or more in MCF10A HER2

https://doi.org/10.1021/acschembio.0c01000
ACS Chem. Biol. 2021, 16, 712−723

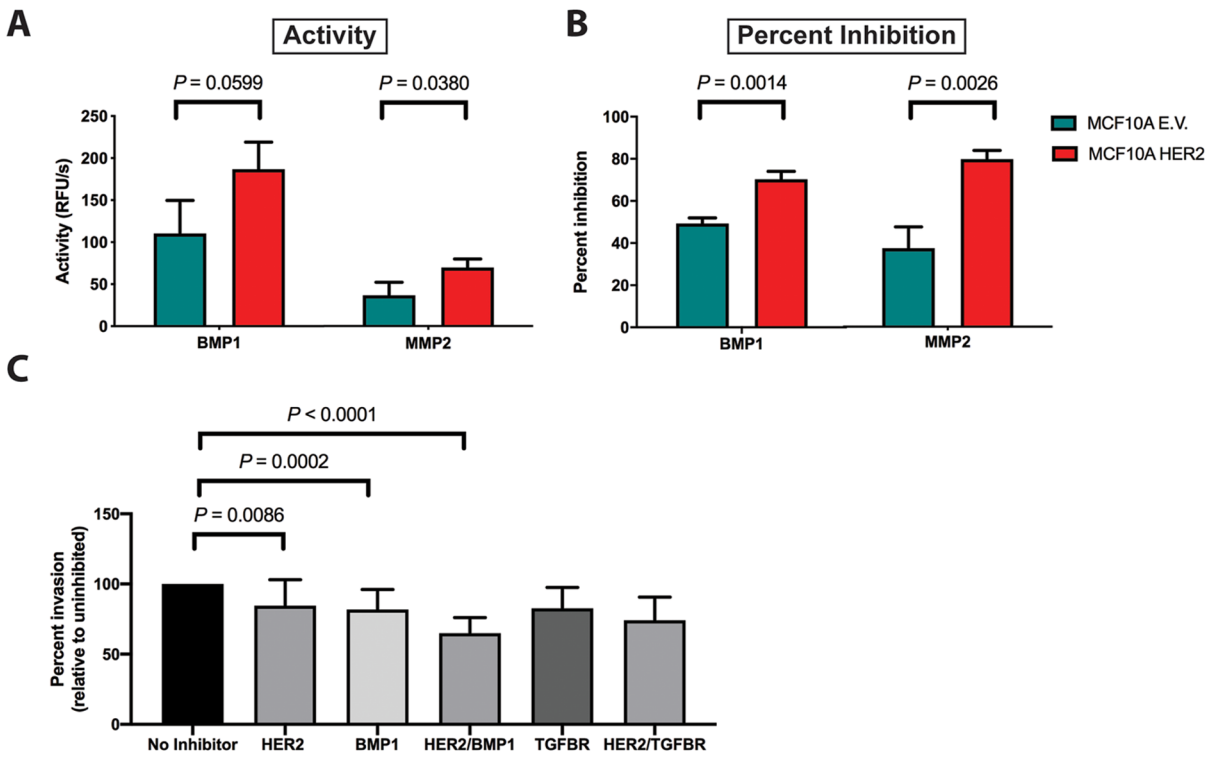

Figure 6. Activity of the metalloprotease BMP1 is upregulated in HER2-expressing cells. HER2 expression results in upregulation of the metalloprotease BMP1 involved in TGF-β signaling. BMP1- and MMP-like protease activity were assayed in conditioned media from MCF10A E.V. (control) and MCF10A HER2 cells using commercially available substrates ± inhibitors. (A) BMP1- (P = 0.0599) and MMP-like (P = 0.0380) activity was upregulated in MCF10A HER2 cells compared to MCF10A control. (B) Activity was inhibited by a BMP1-specific inhibitor (UK-383367) and broad-spectrum metalloprotease inhibitor (batimastat). (C) Inhibition of MCF10A HER2 cells with a HER2 and BMP1 inhibitor resulted in decreased invasion *in vitro* across a basement membrane extract after 24 h (P = 0.0086 for HER2, P = 0.0002 for BMP1, and P < 0.0001 for HER2/BMP1). Mean activity/percent inhibition is reported as the mean RFU of three replicates ± SD. Mean invasion is reported as mean RFU of 12 well replicates ± SD.

overexpression cells (n = 4, P < 0.05) and found in the MSP-MS assay incorporating inhibitors (Table S4) were also completely inhibited by 1,10-P (Figure 5B). While the metalloprotease inhibitor 1,10-P broadly blocked HER2 selective cleavages, some of these cleavages were also inhibited by cysteine protease inhibitor E-64, suggesting that HER2-driven proteolysis is probably not related to a single class of proteases. Taken together, these results show that oncogenic transformation by HER2 results in changes in extracellular proteolysis with differential metalloproteinase activity as the predominant contributor.

HER2 Expression Results in Increased BMP1- and MMP2-like Activity. On the basis of TGF-β signaling activation and predominant metalloproteinase activity, we decided to investigate whether two secreted metalloproteases, BMP1 and MMP2, were also upregulated at the activity level. While it is difficult to definitely match the inhibited cleavages observed in the profiling assay (Figure 5B) with BMP1 and MMP2 due to their broad substrate specificities and likely overlap with other proteases present in the complex mixture, both BMP1 and MMP2 are known to play a critical role in TGF-β signaling activation. Increased expression of BMP1 and not MMP2 was observed by proteomics in conditioned media; however, increased MMP2 expression in HER2-expressing cells has been well documented.[40] In its inactive state, TGF-β is sequestered to the extracellular matrix by covalent linkage to LTBP1; BMP1 cleavage of LTBP1 at two positions then allows for MMP2-mediated release of TGF-β.[30] Conditioned media from MCF10A HER2 overexpression and MCF10A control cells were incubated with commercially available substrates for BMP1 and MMP2. We found BMP1- (P = 0.0599) and MMP-like (P = 0.0380) activity to be upregulated in MCF10A HER2 cells (Figure 6A). Increased activity was confirmed to be inhibited by a BMP1 specific inhibitor (UK-383367) and broad-spectrum metalloprotease inhibitor (batimastat; Figure 6B).

TGF-β signaling has been studied in the context of the increased invasive potential of HER2-overexpressing cells;[35] however, the exact role BMP1 plays in this process has not been elucidated. Therefore, we sought to investigate the functional role of BMP1 in the invasiveness of MCF10A HER2 cells. Cells were treated with CI-1033 (HER2 inhibitor), galunisertib (TGF-β receptor, TGFBR, inhibitor), and UK-383367 (BMP1 inhibitor). Differences in cellular invasion across a basement membrane extract were assessed after 24 h *in vitro*. HER2 inhibition resulted in a 15% decrease (P = 0.0086) in invasion, whereas BMP1 inhibition resulted in an 18% decrease (P = 0.0002) in cell invasion. Importantly, inhibiting HER2 and BMP1 together resulted in a 35% decreased invasion (P < 0.0001; Figure 6C). As expected, TGFBR and TGFBR/HER2 inhibition also showed a significant decrease in invasion, 17% (P = 0.0006) and 26% (P < 0.0001), respectively (Figure 6C). BMP1 and TGFBR inhibition did not have any effect on cell proliferation after 72

https://doi.org/10.1021/acschembio.0c01000
ACS Chem. Biol. 2021, 16, 712−723

h (Figure S6). Taken together, our results support the role of BMP1 in the functional crosstalk between TGF-β and HER2 signaling, possibly through regulation of TGF-β bioavailability.

DISCUSSION

Genome-wide transcriptional analyses of breast tumors and cell lines have been instrumental in elucidating molecular-level differences in cancer, identifying markers of disease progression, and developing predictors of drug response.[7−9] Although there is a strong association between molecular subtypes of breast cancer and prognosis, a significant number of patients present similar morphological or molecular features but have distinct clinical outcomes. For example, endocrine therapy is the treatment of choice for luminal A breast cancer, typically characterized by the presence of the estrogen and progesterone hormone receptors.[41] However, while many luminal A tumors are responsive to hormone therapy such as tamoxifen, a subset of tumors possess intrinsic and/or acquired resistance.[42−44] The heterogeneity observed even in well characterized breast cancer subtypes reflects the need for complementary approaches that more accurately reflect the functional state of tumors. Understanding the correlation between genotype and phenotype has the potential to improve genetic markers currently being explored in precision medicine.[45] Numerous strategies exploiting differential protease activity in cancer are already being explored for improving cancer diagnosis and therapy.[45] Here, we used an unbiased and global substrate profiling strategy coupled with proteomics to identify differences in protease activities in breast cancer subtypes. Using cancer cell lines, we identified functionally distinct subtypes based on differences in protease global substrate specificities within previously defined genetic subtypes. In addition, using an isogenic cell line model of the HER2 subtype, we were able to identify proteases contributing to the oncogenic potential of HER2 through activation of TGF-β signaling.

Basal-like breast tumors are often associated with a more aggressive phenotype.[46] Indeed, previous functional studies assessing the invasion potential of breast cancer subtypes have shown that basal B cell lines are able to invade across a basement membrane barrier more efficiently than luminal cell lines.[9] Consistent with an increase in protease activity associated with cancer aggressiveness,[47] we observed higher proteolytic activity in basal B cell lines compared to luminal cell lines. Leveraging differences in protease activity in breast cancer subtypes can allow for a better understanding of the molecular mechanisms underlying the disease and pave the way for diagnostic development. For example, a recent study has identified differences in protease activity that enable differentiation of pancreatic cysts (nonmucinous vs mucinous) in patient samples, significantly outperforming molecular biomarkers.[48] In addition, activity-based profiling of whole tissue extracts has been used for the optimization and design of fluorescent probes that are specifically activated in the tumor microenvironment.[49]

Previous studies have examined the role of proteases in oncogenic signaling and therapeutic response.[50] For example, proteolytic cleavage of the HER2 extracellular domain by the "sheddase" ADAM10 results in constitutive activation of HER2 signaling.[51] Metalloproteases have been studied in detail both under normal physiological conditions and in cancer with matrix metalloproteases (MMPs) in particular emerging as promising therapeutic targets because of their role in cancer progression.[52,53] However, MMP inhibitors have not been successful in clinical trials, in part due to an incomplete understanding of the complex and multifaced roles that proteases play in oncogenic signaling pathways.[54] Here, we identified BMP1 as one of the metalloproteases differentially upregulated upon HER2 overexpression. Although the family of BMP/TGF-β growth factors has been evaluated in some detail in breast cancer,[55,56] the functional role of BMP1 in this context has not been studied extensively. Our analysis shows an important role for BMP1 in HER2-mediated invasion, possibly through regulation of TGF-β bioavailability. Future analysis of BMP1 activity in breast tumors is required to validate the importance of BMP1 in the HER2 subtype and across the breast cancer disease spectrum.

In summary, we present an unbiased and global approach that can be used to identify functional subtypes of breast cancer based on differences in global proteolytic signatures. In the future, differences in proteolytic activity can be exploited to generate functional probes to further interrogate signaling mechanisms driving the disease. While beyond the scope of this paper, we envision that protease activity may lead to the establishment of functionally relevant activity-based subtypes that have the potential to advance decision-making for cancer diagnosis and treatment.

METHODS

Cell Lines. Breast cancer cell lines: BT-549, BT-474, MDA-MB-231, MDA-MB-435, MDA-MB-436, MDA-MB-453, MDA-MB-468, SK-BR-3, and MDA-MB-231 were purchased from American Tissue Culture Collection (ATCC) and maintained in Dulbecco's modified Eagle's medium (DMEM): high glucose medium, supplemented with 10% Fetal Bovine serum, 1X sodium pyruvate and 1X Pen/Strep. The MCF10A control (Empty Vector) and MCF10A HER2 cell lines were a gift from the laboratory of Sourav Bandyopadhyay at UCSF and generated according to published methods.[57] Cell lines were maintained in 50% DMEM and 50% F-12 (DMEM/F12) medium, supplemented with 5% Horse serum (Invitrogen), 20 ng/mL epidermal growth factor (EGF; Invitrogen), 500 ng/mL hydrocortisone (Sigma), 100 ng/mL Cholera Toxin (Sigma), 10 μg/mL Insulin (Sigma), 2 μg/mL Puromycin (Invitrogen), and 1X Pen/Strep. Cell line identities were continuously authenticated by morphological inspection. Symptoms for mycoplasma contamination were not observed. All cell lines were incubated at 37 °C in a humidified atmosphere of 5% CO_2.

Conditioned Media Preparation for Proteomic and MSP-MS Analysis. Cell lines were grown to approximately 80% confluency at 37 °C in a humidified atmosphere of 5% CO_2. Cells were washed 3−5 times with D-PBS and switched to serum-free DMEM or serum-free DMEM/F12 medium for 20−24 h. Conditioned media were harvested by spinning at 900 rpm for 5 min to pellet cells, and the supernatant was collected. Supernatant was filtered using a 0.45 μm vacuum filtration system. Filtered conditioned media were concentrated immediately or frozen in liquid nitrogen and stored at −80 °C. Conditioned media were concentrated through centrifugation with a 10 kDa molecular weight cutoff (MWCO) spin filter and buffer exchanged into D-PBS, pH 7.4 (10-fold). Protein quantification was done using the Bradford or bicinchoninic acid assay (BCA) method, flash frozen, and stored at −80 °C.

Proteomic Analysis. Conditioned media for proteomics analysis were prepared following previously published methods for proteomics.[58] Trypsin-derived peptides were subjected to peptide sequencing by LC-MS/MS. Protein identification and label-free quantification were carried out in MaxQuant[59] and analyzed using Perseus.[60] Differential protein expression and statistical analysis were performed using the Bioconductor package: Proteus.[61]

Peptide sequencing for cell lines in Table 1 was carried out by LC-MS/MS on an LTQ-Orbitrap XL mass spectrometer (Thermo) with a

https://doi.org/10.1021/acschembio.0c01000
ACS Chem. Biol. 2021, 16, 712−723

nanoACQUITY ultraperformance LC (UPLC) system (Waters) and an EASY-Spray ion source (Thermo) using previously described methods for data acquisition.[58] Peptide sequencing for MCF10A cell lines was carried out by LC-MS/MS on an LTQ-Orbitrap Velos mass spectrometer (Thermo) with a nanoACQUITY ultraperformance LC (UPLC; Waters) and an EASY-Spray ion source (Thermo). Sample loading in the UPLC system was conducted at a flow rate of 600 nL/min for 20 min, followed by peptide separation with a linear gradient from 2 to 50% acetonitrile (0.1% formic acid). Survey scans were recorded over a mass range of 350 to 1500 m/z, with the six most intense precursor ions fragmented by higher-energy collisional dissociation (HCD) for tandem MS analysis.

Multiplex Substrate Profiling by Mass Spectrometry (MSP-MS). Global protease activity was determined by assaying matched conditioned media using the MSP-MS assay as previously described.[58] Sequences for the 228-member synthetic peptide library used in the MSP-MS assay have been previously published.[19] Briefly, matched conditioned media from breast cancer cell lines, MCF10A control and MCF10 HER2 were diluted to 50 μg/mL (1X) in assay buffer (PBS, pH 7.4) and preincubated for 30 min on ice with or without inhibitor. Protease inhibitor assays were carried out using the following final concentrations: 1 mM 4-(2-Aminoethyl)benzenesulfonyl fluoride hydrochloride (AEBSF; Sigma), 2 μM E-64 (Sigma), 2 μM Bestatin (Sigma), 1 mM 1,10-Phenanthroline (1,10-P; Sigma), or DMSO (no inhibitor).

Peptide sequencing by LC-MS/MS was carried out on an LTQ-Orbitrap XL mass spectrometer (Thermo) with a nanoACQUITY ultraperformance LC (UPLC) system (Waters) and an EASY-Spray ion source (Thermo). Data acquisition was performed using previously described methods.[58]

Clustering Analysis. Cluster analysis was performed using the coupled two-way clustering algorithm implemented in *biclust* package in R programming language.[21] Each amino acid of a peptide was encoded using three Hellberg z-scores or descriptors.[62] These scores are represented by the first three principal components of the 20 physicochemical properties of the 20 amino acids. The first principal component is dominated by the hydrophilicity or polarity of the amino acid and the second principal component is related to the size of the amino acid. Thus, each 8-mer peptide (P4−P4') represented by $3 \times 8 = 24$ descriptors. Prior to cluster analysis, descriptors were centered and scaled. Centering was done by subtracting the means of each descriptor and scaling was done by dividing the (centered) descriptor values by their standard deviations. Distances between encoded peptides were calculated using Euclidean metric.

Cell Viability Assays. The effects of CI-1033 (HER2; Selleckchem), Galunisertib (TGFBR; Selleckchem), and UK-383367 (BMP1; Selleckchem) on cell viability were assessed using Cell Titer-Glo (Promega). Cells were plated in black-walled, clear bottom 96-well plates at 5,000 per well and allowed to adhere overnight at 37 °C in a humidified atmosphere of 5% CO_2. Varying concentrations of inhibitors were then added, and cells were incubated for 3 days. Cell Titer-Glo was added according to manufacturer's protocol and the luminescent signal was measured using a SpectraMax iD5 Hybrid Multi-Mode Microplate Reader with excitation at 485 nm and emission at 520 nm. For all cellular assays, dose−response curves were generated using GraphPad Prism version 8.4 (GraphPad Software).

Cell Proliferation and Invasion Assays. To determine cell proliferation, 2,000 cells were plated per well in 96-well plates and frozen at −80 °C at given time points (24−72 h). Cell proliferation was determined as an increase in fluorescence using the CyQUANT Cell Proliferation Assay kit (Invitrogen) and reading in a BioTek Synergy H4 Hybrid Multi-Mode Microplate Reader with excitation at 485 nm and emission at 520 nm. The invasion potential of MCF10A EV and MCF10A HER2 cells was assessed using a 1X basement membrane extract (BME) coated Boyden chamber according to manufacturer's protocol (Trevigen). Optimal seeding density was determined to be 50,000 cells per well for each cell line. For inhibitor invasion assay, inhibitors were added to top and bottom wells in corresponding media at concentrations not toxic to the cells. The following concentrations were used: 100 nM CI-1033, 1 μM UK-383367 (Selleckchem), and 1 μM Galunisertib (Selleckchem). The number of invaded cells in the lower chamber was determined per manufacturer's protocol by fluorescence measurement using a SpectraMax iD5 Hybrid Multi-Mode Microplate Reader with excitation at 485 nm and emission at 520 nm.

Western Blots. Cells were harvested and lysed in RIPA buffer (Pierce), supplemented with a Protease/Phosphatase inhibitor cocktail (100X) following standard sample preparation protocol (Abcam). Protein concentration of cell lysates were determined by BCA. Cell lysate (30−50 μg) was run on 4−12% SurePAGE Bis-Tris polyacrylamide gel (GenScript). Proteins were transferred onto nitrocellulose membrane (Life Technologies) using the iBlot Dry Blotting System (Life Technologies). Membranes were blocked for at least 1 h in 5% nonfat dry milk in Tris-buffered saline with 0.1% Tween-20 (TBS-T) at 4 °C. All primary antibodies were prepared in 5% nonfat dry milk in TBS-T (1:1000 dilution) and incubated overnight at 4 °C. GAPDH was used as a loading control (1:10000). LI-COR secondary antibodies (1:10000) were used to simultaneously measure protein of interest and GAPDH levels. Signal was detected using the Odyssey Infrared Imaging System (LI-COR Biosciences). Densitometry analysis was done using ImageJ (National Institute of Health).

Protease Activity Assays. Activity assays with commercially available fluorogenic substrates for BMP1 (Catalog No. ES007, R&D Systems) and MMP2 (Catalog No. SCP0192, Sigma) were performed for 1 h in black 96-well round-bottom plates (Catalog No. 3356, Costar) using a BioTek Synergy H4 Hybrid Multi-Mode Microplate Reader set to 37 °C with excitation at 320 nm and emission at 405 nm. Activity assays were performed with 10 μM substrate and 50 μg/mL conditioned media. For inhibitor assays, conditioned media were preincubated with 10 μM UK-383367 (Selleckchem) or 10 μM Batimastat (Selleckchem) for 30 min on ice. Activity assays were carried out in PBS buffer, pH 7.4, supplemented with 0.01% Brij 35. Relative fluorescence units (RFUs) were calculated using Gen5 software. Activity is reported as mean RFU values ± SD of three replicates.

Statistical Analysis. Statistical analysis was carried out in Proteus[60] for proteomic analysis and in GraphPad Prism version 8.4 (GraphPad Software Inc.) for all other experiments. Statistical significance was calculated using unpaired two-tailed t test. For densitometry analysis, the mean value is reported ± standard deviation (SD) of three replicates. For the cell proliferation assay, the mean value is reported ± SD of four replicates. For *in vitro* invasion assays, the mean value is reported ± SD of six wells or 12 wells (Figure 3C, Figure 6C, respectively). For protease activity assays, mean activity is reported ± SD for three replicates.

■ ASSOCIATED CONTENT

Supporting Information

The Supporting Information is available free of charge at https://pubs.acs.org/doi/10.1021/acschembio.0c01000.

Analysis of proteases and protease inhibitors differentially expressed at the gene and protein levels; global protease substrate specificity profiles for a panel of nine breast cancer cell lines, MCF10A E.V. (control), and MCF10A HER2-expressing cell lines; and cell proliferation of MCF10A control and MCF10A HER2-expressing cell lines (PDF)

Proteomic analysis of extracellular proteins in nine breast cancer cell lines (XLSX)

Global protease profiling in breast cancer subtypes (XLSX)

Proteomic analysis of extracellular proteins in an isogenic HER2 cell line model (XLSX)

Global protease profiling in an isogenic HER2 cell line model (XLSX)

https://doi.org/10.1021/acschembio.0c01000
ACS Chem. Biol. 2021, 16, 712−723

AUTHOR INFORMATION

Corresponding Author

Charles S. Craik − *Department of Pharmaceutical Chemistry, University of California—San Francisco, San Francisco, California 94158, United States;* orcid.org/0000-0001-7704-9185; Phone: (415) 476 8146; Email: charles.craik@ucsf.edu

Authors

Eugenia C. Salcedo − *Chemistry and Chemical Biology Graduate Program, University of California—San Francisco, San Francisco, California 94158, United States*

Michael B. Winter − *Department of Pharmaceutical Chemistry, University of California—San Francisco, San Francisco, California 94158, United States*

Natalia Khuri − *Department of Bioengineering and Therapeutic Sciences, University of California—San Francisco, San Francisco, California 94158, United States*

Giselle M. Knudsen − *Department of Pharmaceutical Chemistry, University of California—San Francisco, San Francisco, California 94158, United States*

Andrej Sali − *Department of Bioengineering and Therapeutic Sciences, University of California—San Francisco, San Francisco, California 94158, United States;* orcid.org/0000-0003-0435-6197

Complete contact information is available at: https://pubs.acs.org/10.1021/acschembio.0c01000

Notes

The authors declare no competing financial interest.

ACKNOWLEDGMENTS

Mass spectrometry was performed in collaboration with the UCSF Mass Spectrometry Facility directed by A. Burlingame. MCF10A EV and MCF10A HER2 cell lines were kind gifts from S. Bandyopadhyay. We thank A. Wiita, D. Ruggero, and F. Caiazza for critical reading of the manuscript, suggestions, and comments, and we thank A. Lourenço for providing assistance, helpful insights, and the design of the supplementary front cover graphic. This study was supported by National Institutes of Health (NIH) grants R21CA186077 (to C.S.C. and A.S.) and P41GM103481 (UCSF Mass Spectrometry Facility). E.C.S. was supported by NIH training grant R25GM056847 and the Howard Hughes Medical Institute Gilliam Fellowship for Advanced Study. M.B.W. was supported by NIH postdoctoral fellowship F32CA168150.

REFERENCES

(1) Subramaniam, D. S., and Isaacs, C. (2005) Utilizing Prognostic and Predictive Factors in Breast Cancer. *Curr. Treat. Options in Oncol.* 6 (2), 147−159.

(2) Cao, S.-S., and Lu, C.-T. (2016) Recent Perspectives of Breast Cancer Prognosis and Predictive Factors (Review). *Oncol. Lett.* 12 (5), 3674−3678.

(3) Slamon, D. J., Clark, G. M., Wong, S. G., Levin, W. J., Ullrich, A., and McGuire, W. L. (1987) Human Breast Cancer: Correlation of Relapse and Survival with Amplification of the HER-2/Neu Oncogene. *Science* 235 (4785), 177−182.

(4) Subik, K., Lee, J.-F., Baxter, L., Strzepek, T., Costello, D., Crowley, P., Xing, L., Hung, M.-C., Bonfiglio, T., Hicks, D. G., and Tang, P. (2010) The Expression Patterns of ER, PR, HER2, CK5/6, EGFR, Ki-67 and AR by Immunohistochemical Analysis in Breast Cancer Cell Lines. *Breast Cancer (Auckl)* 4, 35−41.

(5) Lawrence, R. T., Perez, E. M., Hernández, D., Miller, C. P., Haas, K. M., Irie, H. Y., Lee, S.-I., Blau, C. A., and Villén, J. (2015) The Proteomic Landscape of Triple-Negative Breast Cancer. *Cell Rep.* 11 (4), 630−644.

(6) Gown, A. M. (2008) Current Issues in ER and HER2 Testing by IHC in Breast Cancer. *Mod. Pathol.* 21 (S2), S8−S15.

(7) Perou, C. M., Jeffrey, S. S., van de Rijn, M., Rees, C. A., Eisen, M. B., Ross, D. T., Pergamenschikov, A., Williams, C. F., Zhu, S. X., Lee, J. C. F., Lashkari, D., Shalon, D., Brown, P. O., and Botstein, D. (1999) Distinctive Gene Expression Patterns in Human Mammary Epithelial Cells and Breast Cancers. *Proc. Natl. Acad. Sci. U. S. A.* 96 (16), 9212−9217.

(8) Sorlie, T., Perou, C. M., Tibshirani, R., Aas, T., Geisler, S., Johnsen, H., Hastie, T., Eisen, M. B., van de Rijn, M., Jeffrey, S. S., Thorsen, T., Quist, H., Matese, J. C., Brown, P. O., Botstein, D., Lonning, P. E., and Borresen-Dale, A.-L. (2001) Gene Expression Patterns of Breast Carcinomas Distinguish Tumor Subclasses with Clinical Implications. *Proc. Natl. Acad. Sci. U. S. A.* 98 (19), 10869−10874.

(9) Neve, R. M., Chin, K., Fridlyand, J., Yeh, J., Baehner, F. L., Fevr, T., Clark, L., Bayani, N., Coppe, J.-P., Tong, F., Speed, T., Spellman, P. T., DeVries, S., Lapuk, A., Wang, N. J., Kuo, W.-L., Stilwell, J. L., Pinkel, D., Albertson, D. G., Waldman, F. M., McCormick, F., Dickson, R. B., Johnson, M. D., Lippman, M., Ethier, S., Gazdar, A., and Gray, J. W. (2006) A Collection of Breast Cancer Cell Lines for the Study of Functionally Distinct Cancer Subtypes. *Cancer Cell* 10 (6), 515−527.

(10) LeBeau, A. M., Duriseti, S., Murphy, S. T., Pepin, F., Hann, B., Gray, J. W., VanBrocklin, H. F., and Craik, C. S. (2013) Targeting UPAR with Antagonistic Recombinant Human Antibodies in Aggressive Breast Cancer. *Cancer Res.* 73 (7), 2070−2081.

(11) Duffy, M. J., McGowan, P. M., Harbeck, N., Thomssen, C., and Schmitt, M. (2014) UPA and PAI-1 as Biomarkers in Breast Cancer: Validated for Clinical Use in Level-of-Evidence-1 Studies. *Breast Cancer Res.* 16 (4), 1−10.

(12) López-Otín, C., and Bond, J. S. (2008) Proteases: Multifunctional Enzymes in Life and Disease. *J. Biol. Chem.* 283 (45), 30433−30437.

(13) Andreasen, P. A., Egelund, R., and Petersen, H. H. (2000) The Plasminogen Activation System in Tumor Growth, Invasion, and Metastasis. *Cell. Mol. Life Sci.* 57 (1), 25−40.

(14) Sevenich, L., and Joyce, J. A. (2014) Pericellular Proteolysis in Cancer. *Genes Dev.* 28 (21), 2331−2347.

(15) Skrzydlewska, E., Sulkowska, M., Koda, M., and Sulkowski, S. (2005) Proteolytic-Antiproteolytic Balance and Its Regulation in Carcinogenesis. *World J. Gastroenterol* 11 (9), 1251−1266.

(16) LeBeau, A. M., Lee, M., Murphy, S. T., Hann, B. C., Warren, R. S., Delos Santos, R., Kurhanewicz, J., Hanash, S. M., VanBrocklin, H. F., and Craik, C. S. (2013) Imaging a Functional Tumorigenic Biomarker in the Transformed Epithelium. *Proc. Natl. Acad. Sci. U. S. A.* 110 (1), 93−98.

(17) Vasiljeva, O., Hostetter, D. R., Moore, S. J., and Winter, M. B. (2019) The Multifaceted Roles of Tumor-Associated Proteases and Harnessing Their Activity for Prodrug Activation. *Biol. Chem.* 400 (8), 965−977.

(18) O'Donoghue, A. J., Eroy-Reveles, A. A., Knudsen, G. M., Ingram, J., Zhou, M., Statnekov, J. B., Greninger, A. L., Hostetter, D. R., Qu, G., Maltby, D. A., Anderson, M. O., DeRisi, J. L., McKerrow, J. H., Burlingame, A. L., and Craik, C. S. (2012) Global Identification of Peptidase Specificity by Multiplex Substrate Profiling. *Nat. Methods* 9 (11), 1095−1100.

(19) Winter, M. B., La Greca, F., Arastu-Kapur, S., Caiazza, F., Cimermancic, P., Buchholz, T. J., Anderl, J. L., Ravalin, M., Bohn, M. F., Sali, A., O'Donoghue, A. J., and Craik, C. S. (2017) Immunoproteasome Functions Explained by Divergence in Cleavage Specificity and Regulation. *eLife* 6, e27364.

(20) Prasad, V. V., and Gopalan, R. O. (2015) Continued Use of MDA-MB-435, a Melanoma Cell Line, as a Model for Human Breast Cancer, Even in Year, 2014. *npj Breast Cancer* 1 (1), 1−2.

(21) Getz, G., Levine, E., and Domany, E. (2000) Coupled Two-Way Clustering Analysis of Gene Microarray Data. *Proc. Natl. Acad. Sci. U. S. A. 97* (22), 12079−12084.
(22) Colaert, N., Helsens, K., Martens, L., Vandekerckhove, J., and Gevaert, K. (2009) Improved Visualization of Protein Consensus Sequences by IceLogo. *Nat. Methods 6* (11), 786−787.
(23) Wang, S. E., Yu, Y., Criswell, T. L., DeBusk, L. M., Lin, P. C., Zent, R., Johnson, D. H., Ren, X., and Arteaga, C. L. (2010) Oncogenic Mutations Regulate Tumor Microenvironment through Induction of Growth Factors and Angiogenic Mediators. *Oncogene 29* (23), 3335−3348.
(24) Yarden, Y., and Sliwkowski, M. X. (2001) Untangling the ErbB Signalling Network. *Nat. Rev. Mol. Cell Biol. 2* (2), 127−137.
(25) Frixen, U. H., Behrens, J., Sachs, M., Eberle, G., Voss, B., Warda, A., Löchner, D., and Birchmeier, W. (1991) E-Cadherin-Mediated Cell-Cell Adhesion Prevents Invasiveness of Human Carcinoma Cells. *J. Cell Biol. 113* (1), 173−185.
(26) Conacci-Sorrell, M., Zhurinsky, J., and Ben-Ze'ev, A. (2002) The Cadherin-Catenin Adhesion System in Signaling and Cancer. *J. Clin. Invest. 109* (8), 987−991.
(27) Giunciuglio, D., Culty, M., Fassina, G., Masiello, L., Melchiori, A., Paglialunga, G., Arand, G., Ciardiello, F., Basolo, F., Thompson, E. W., and Albini, A. (1995) Invasive Phenotype of MCF10A Cells Overexpressing C-Ha-ras and C-erbB-2 Oncogenes. *Int. J. Cancer 63* (6), 815−822.
(28) Nistala, H., Lee-Arteaga, S., Smaldone, S., Siciliano, G., Carta, L., Ono, R. N., Sengle, G., Arteaga-Solis, E., Levasseur, R., Ducy, P., Sakai, L. Y., Karsenty, G., and Ramirez, F. (2010) Fibrillin-1 and −2 Differentially Modulate Endogenous TGF-β and BMP Bioavailability during Bone Formation. *J. Cell Biol. 190* (6), 1107−1121.
(29) Miyazono, K., Olofsson, A., Colosetti, P., and Heldin, C. H. (1991) A Role of the Latent TGF-Beta 1-Binding Protein in the Assembly and Secretion of TGF-Beta 1. *EMBO J. 10* (5), 1091−1101.
(30) Ge, G., and Greenspan, D. S. (2006) BMP1 Controls TGFβ1 Activation via Cleavage of Latent TGFβ-Binding Protein. *J. Cell Biol. 175* (1), 111−120.
(31) Xu, J., Acharya, S., Sahin, O., Zhang, Q., Saito, Y., Yao, J., Wang, H., Li, P., Zhang, L., Lowery, F. J., Kuo, W.-L., Xiao, Y., Ensor, J., Sahin, A. A., Zhang, X. H.-F., Hung, M.-C., Zhang, J. D., and Yu, D. (2015) 14−3-3ζ Turns TGF-β's Function from Tumor Suppressor to Metastasis Promoter in Breast Cancer by Contextual Changes of Smad Partners from P53 to Gli2. *Cancer Cell 27* (2), 177−192.
(32) Delolme, F., Anastasi, C., Alcaraz, L. B., Mendoza, V., Vadon-Le Goff, S., Talantikite, M., Capomaccio, R., Mevaere, J., Fortin, L., Mazzocut, D., Damour, O., Zanella-Cléon, I., Hulmes, D. J. S., Overall, C. M., Valcourt, U., Lopez-Casillas, F., and Moali, C. (2015) Proteolytic Control of TGF-β Co-Receptor Activity by BMP-1/Tolloid-like Proteases Revealed by Quantitative ITRAQ Proteomics. *Cell. Mol. Life Sci. 72* (5), 1009−1027.
(33) Rousselle, P., and Scoazec, J. Y. (2019) Laminin 332 in Cancer: When the Extracellular Matrix Turns Signals from Cell Anchorage to Cell Movement. *Semin. Cancer Biol. 62*, 149.
(34) Chow, A., Arteaga, C. L., and Wang, S. E. (2011) When Tumor Suppressor TGFβ Meets the HER2 (ERBB2) Oncogene. *J. Mammary Gland Biol. Neoplasia 16* (2), 81−88.
(35) Wang, S. E., Xiang, B., Guix, M., Olivares, M. G., Parker, J., Chung, C. H., Pandiella, A., and Arteaga, C. L. (2008) Transforming Growth Factor Beta Engages TACE and ErbB3 to Activate Phosphatidylinositol-3 Kinase/Akt in ErbB2-Overexpressing Breast Cancer and Desensitizes Cells to Trastuzumab. *Mol. Cell. Biol. 28* (18), 5605−5620.
(36) Wang, T., Gorgoglione, B., Maehr, T., Holland, J. W., Vecino, J. L. G., Wadsworth, S., and Secombes, C. J. (2011) The Functional Crosstalk between HER2 Tyrosine Kinase and TGF-β Signaling in Breast Cancer Malignancy. *J. Signal Transduct 2011*, 804236.
(37) Bydoun, M., Sterea, A., Weaver, I. C. G., Bharadwaj, A. G., and Waisman, D. M. (2018) A Novel Mechanism of Plasminogen Activation in Epithelial and Mesenchymal Cells. *Sci. Rep. 8* (1), 14091.
(38) Allgayer, H., Babic, R., Gruetzner, K. U., Tarabichi, A., Schildberg, F. W., and Heiss, M. M. (2000) C-ErbB-2 Is of Independent Prognostic Relevance in Gastric Cancer and Is Associated With the Expression of Tumor-Associated Protease Systems. *J. Clin. Oncol. 18* (11), 2201−2209.
(39) Pellikainen, J. M., Ropponen, K. M., Kataja, V. V., Kellokoski, J. K., Eskelinen, M. J., and Kosma, V.-M. (2004) Expression of Matrix Metalloproteinase (MMP)-2 and MMP-9 in Breast Cancer with a Special Reference to Activator Protein-2, HER2, and Prognosis. *Clin. Cancer Res. 10* (22), 7621−7628.
(40) Kim, I.-Y., Yong, H.-Y., Kang, K. W., and Moon, A. (2009) Overexpression of ErbB2 Induces Invasion of MCF10A Human Breast Epithelial Cells via MMP-9. *Cancer Lett. 275* (2), 227−233.
(41) Ciriello, G., Sinha, R., Hoadley, K. A., Jacobsen, A. S., Reva, B., Perou, C. M., Sander, C., and Schultz, N. (2013) The Molecular Diversity of Luminal A Breast Tumors. *Breast Cancer Res. Treat. 141* (3), 409−420.
(42) Higgins, M. J., and Stearns, V. (2009) Understanding Resistance to Tamoxifen in Hormone Receptor-Positive Breast Cancer. *Clin. Chem. 55* (8), 1453−1455.
(43) Ring, A., and Dowsett, M. (2004) Mechanisms of Tamoxifen Resistance. *Endocr.-Relat. Cancer 11* (4), 643−658.
(44) Poudel, P., Nyamundanda, G., Patil, Y., Cheang, M. C. U., and Sadanandam, A. (2019) Heterocellular Gene Signatures Reveal Luminal-A Breast Cancer Heterogeneity and Differential Therapeutic Responses. *npj Breast Cancer 5* (1), 21.
(45) Dudani, J. S., Warren, A. D., and Bhatia, S. N. (2018) Harnessing Protease Activity to Improve Cancer Care. *Annual Review of Cancer Biology 2* (1), 353−376.
(46) Bertucci, F., Finetti, P., and Birnbaum, D. (2012) Basal Breast Cancer: A Complex and Deadly Molecular Subtype. *Curr. Mol. Med. 12* (1), 96−110.
(47) Duffy, M. J. (1992) The Role of Proteolytic Enzymes in Cancer Invasion and Metastasis. *Clin. Exp. Metastasis 10* (3), 145−155.
(48) Ivry, S. L., Sharib, J. M., Dominguez, D. A., Roy, N., Hatcher, S. E., Yip-Schneider, M. T., Schmidt, C. M., Brand, R. E., Park, W. G., Hebrok, M., Kim, G. E., O'Donoghue, A. J., Kirkwood, K. S., and Craik, C. S. (2017) Global Protease Activity Profiling Provides Differential Diagnosis of Pancreatic Cysts. *Clin. Cancer Res. 23* (16), 4865−4874.
(49) Tholen, M., Yim, J. J., Groborz, K., Yoo, E., Martin, B. A., Berg, N. S., Drag, M., and Bogyo, M. (2020) Design of Optical-Imaging Probes by Screening of Diverse Substrate Libraries Directly in Disease-Tissue Extracts. *Angew. Chem., Int. Ed. 59* (43), 19143−19152.
(50) Borrell-Pagès, M., Rojo, F., Albanell, J., Baselga, J., and Arribas, J. (2003) TACE Is Required for the Activation of the EGFR by TGF-α in Tumors. *EMBO J. 22* (5), 1114−1124.
(51) Liu, P. C. C., Liu, X., Li, Y., Covington, M., Wynn, R., Huber, R., Hillman, M., Yang, G., Ellis, D., Marando, C., Katiyar, K., Bradley, J., Abremski, K., Stow, M., Rupar, M., Zhuo, J., Li, Y.-L., Lin, Q., Burns, D., Xu, M., Zhang, C., Qian, D.-Q., He, C., Sharief, V., Weng, L., Agrios, C., Shi, E., Metcalf, B., Newton, R., Friedman, S., Yao, W., Scherle, P., Hollis, G., and Burn, T. C. (2006) Identification of ADAM10 as a Major Source of HER2 Ectodomain Sheddase Activity in HER2 Overexpressing Breast Cancer Cells. *Cancer Biol. Ther. 5* (6), 657−664.
(52) Cathcart, J., Pulkoski-Gross, A., and Cao, J. (2015) Targeting Matrix Metalloproteinases in Cancer: Bringing New Life to Old Ideas. *Genes & Diseases 2* (1), 26−34.
(53) Egeblad, M., and Werb, Z. (2002) New Functions for the Matrix Metalloproteinases in Cancer Progression. *Nat. Rev. Cancer 2* (3), 161−174.
(54) Turk, B. (2006) Targeting Proteases: Successes, Failures and Future Prospects. *Nat. Rev. Drug Discovery 5* (9), 785−799.
(55) Owens, P., Pickup, M. W., Novitskiy, S. V., Giltnane, J. M., Gorska, A. E., Hopkins, C. R., Hong, C. C., and Moses, H. L. (2015) Inhibition of BMP Signaling Suppresses Metastasis in Mammary Cancer. *Oncogene 34* (19), 2437−2449.

https://doi.org/10.1021/acschembio.0c01000
ACS Chem. Biol. 2021, 16, 712−723

(56) Jiang, R., Ding, L., Zhou, J., Huang, C., Zhang, Q., Jiang, Y., Liu, J., Yan, Q., Zhen, X., Sun, J., Yan, G., and Sun, H. (2017) BMP-2 Induces EMT and Breast Cancer Stemness through Rb and CD44. *Cell Death Discovery* 3 (1), 1−12.
(57) Martins, M. M., Zhou, A. Y., Corella, A., Horiuchi, D., Yau, C., Rakhshandehroo, T., Gordan, J. D., Levin, R. S., Johnson, J., Jascur, J., Shales, M., Sorrentino, A., Cheah, J., Clemons, P. A., Shamji, A. F., Schreiber, S. L., Krogan, N. J., Shokat, K. M., McCormick, F., Goga, A., and Bandyopadhyay, S. (2015) Linking Tumor Mutations to Drug Responses via a Quantitative Chemical−Genetic Interaction Map. *Cancer Discovery* 5 (2), 154−167.
(58) Winter, M. B., Salcedo, E. C., Lohse, M. B., Hartooni, N., Gulati, M., Sanchez, H., Takagi, J., Hube, B., Andes, D. R., Johnson, A. D., Craik, C. S., and Nobile, C. J. (2016) Global Identification of Biofilm-Specific Proteolysis in Candida Albicans. *mBio* 7 (5), e01514−16.
(59) Tyanova, S., Temu, T., and Cox, J. (2016) The MaxQuant Computational Platform for Mass Spectrometry-Based Shotgun Proteomics. *Nat. Protoc.* 11 (12), 2301−2319.
(60) Tyanova, S., and Cox, J. (2018) Perseus: A Bioinformatics Platform for Integrative Analysis of Proteomics Data in Cancer Research. *Methods Mol. Biol. 1711*, 133−148.
(61) Gierlinski, M., Gastaldello, F., Cole, C., and Barton, G. J. Proteus: An R Package for Downstream Analysis of MaxQuant Output 2018. *bioRxiv* 416511, (March 26, 2020).
(62) Hellberg, S., Sjöström, M., Skagerberg, B., and Wold, S. (1987) Peptide Quantitative Structure-Activity Relationships, a Multivariate Approach. *J. Med. Chem.* 30 (7), 1126−1135.

https://doi.org/10.1021/acschembio.0c01000
ACS Chem. Biol. 2021, 16, 712−723